PAPER • OPEN ACCESS

Onlay-graft of 3D printed Kagome-structure PCL scaffold incorporated with rhBMP-2 based on hyaluronic acid hydrogel

To cite this article: Jeong-Kui Ku *et al* 2021 *Biomed. Mater.* **16** 055004

View the article online for updates and enhancements.

You may also like

- The Variability of the Black Hole Image in M87 at the Dynamical Timescale
Kaushik Satapathy, Dimitrios Psaltis, Feryal Özel et al.
- First BISTRO Observations of the Dark Cloud Taurus L1495A-B10: The Role of the Magnetic Field in the Earliest Stages of Low-mass Star Formation
Derek Ward-Thompson, Janik Karoly, Kate Pattle et al.
- First M87 Event Horizon Telescope Results. I. The Shadow of the Supermassive Black Hole
The Event Horizon Telescope Collaboration, Kazunori Akiyama, Antxon Alberdi et al.

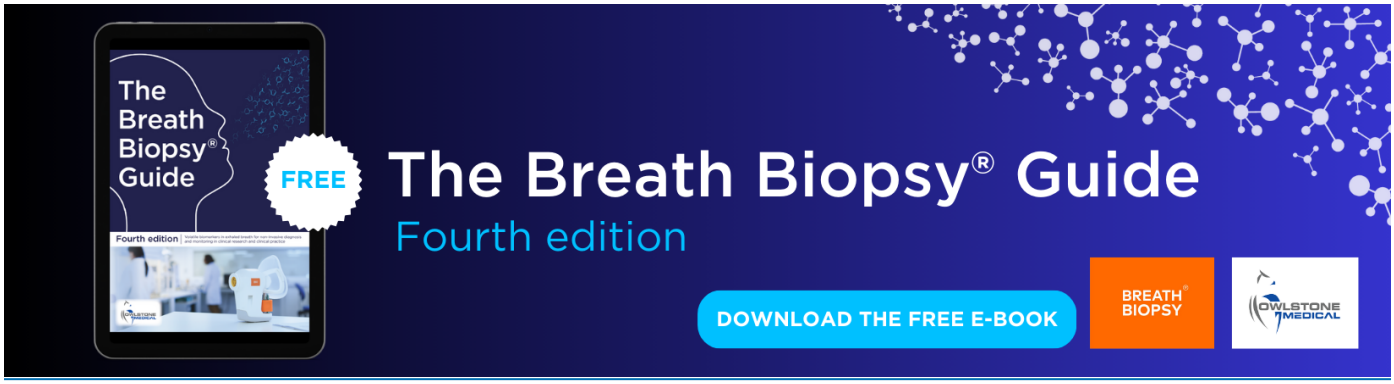

This content was downloaded from IP address 116.89.178.139 on 15/03/2024 at 07:49

IOP Publishing Biomed. Mater. 16 (2021) 055004 https://doi.org/10.1088/1748-605X/ac0f47

Biomedical Materials

CrossMark

OPEN ACCESS

RECEIVED
8 April 2021

REVISED
5 June 2021

ACCEPTED FOR PUBLICATION
28 June 2021

PUBLISHED
14 July 2021

Original content from this work may be used under the terms of the Creative Commons Attribution 4.0 licence.

Any further distribution of this work must maintain attribution to the author(s) and the title of the work, journal citation and DOI.

PAPER

Onlay-graft of 3D printed Kagome-structure PCL scaffold incorporated with rhBMP-2 based on hyaluronic acid hydrogel

Jeong-Kui Ku[1,2,9], Kang-Gon Lee[3,9], Min-Soo Ghim[4,9], Young-Kyun Kim[5], Sang-Hyug Park[6], Yongdoo Park[3], Young-Sam Cho[4,7] and Bu-Kyu Lee[1,8,*]

[1] Department of Oral and Maxillofacial Surgery, Asan Medical Center, College of Medicine, University of Ulsan, 88, Olympic-ro 43-gil, Songpa-gu, Seoul 05505, Republic of Korea
[2] Department of Oral and Maxillofacial Surgery, Gangnam Severance Hospital, Yonsei University College of Dentistry, 211 Eonju-ro, Gandnam-gu, Seoul 06273, Republic of Korea
[3] Department of Biomedical Sciences, College of Medicine, Korea University, Seoul 02841, Republic of Korea
[4] Department of Mechanical Engineering, Wonkwang University, 460 Iksandae-ro, Iksan, Jeonbuk 54538, Republic of Korea
[5] Department of Oral and Maxillofacial Surgery, Section of Dentistry, Seoul University Bundang Hospital, 81, Saemaul-ro 117, Bundang-gu, Seongnam-si 13634, Republic of Korea
[6] Department of Biomedical Engineering, Pukyong National Universtiy, 45, Yongso-Ro, Nam-Gu, Busan, Republic of Korea
[7] Department of Mechanical and Design Engineering, Wonkwang University, 460 Iksandae-ro, Iksan, Jeonbuk 54538, Republic of Korea
[8] Department of Oral and Maxillofacial Surgery, Biomedical Engineering Research Center, Asan Institute for Life Sciences, Asan Medical Center, College of Medicine, University of Ulsan, 88, Olympic-ro 43-gil, Songpa-gu, Seoul 05505, Republic of Korea
[9] These authors contributed equally to this work.
* Author to whom any correspondence should be addressed.

E-mail: Bukyu.lee@gmail.com

Keywords: 3D printing, onlay-graft, bone morphogenetic protein-2, polycaprolactone, scaffolds, hyaluronic acid

Abstract

The onlay-graft, one of the most difficult graft conditions, is used for diverse clinical conditions, including plastic and dental surgery. The graft should withstand continuous pressure from overlying tissues and have excellent bone formation capability in a limited bone contact situation. We recently developed a 3D printed Kagome-structured polycaprolactone (PCL) scaffold that has a stronger mechanical property. This study evaluated the clinical feasibility of this scaffold for onlay-graft use. The value of the scaffold containing recombinant human bone morphogenetic protein-2 in a hyaluronate-based hydrogel (rhBMP-2/HA) to enhance bone regeneration was also assessed. 3D-printed Kagome-PCL scaffolds alone ($n = 12$, group I) or loaded with rhBMP-2/HA ($n = 12$, group II) were grafted using a rat calvarial onlay-graft model. Following sacrifice at 2, 4, and 8 weeks, all 3D-printed Kagome-PCL scaffolds were accurately positioned and firmly integrated to the recipient bone. Micro-computed tomography and histology analyses revealed a constant height of the scaffolds over time in all animals. New bone grew into the scaffolds in both groups, but with greater volume in group II. These results suggest the promising clinical feasibility of the 3D-printed Kagome-PCL scaffold for onlay-graft use and it could substitute the conventional onlay-graft in the plastic and dental reconstructive surgery in the near future.

1. Introduction

Autologous bone graft is still considered the gold standard for bone grafts, reflecting its osteogenesis, osteoinduction, and osteoconduction properties [1]. Disadvantages of autografts include extended healing time and need for additional surgeries. To overcome these limitations, bone tissue engineering has sought to temporarily substitute the extracellular matrix. The influence of several bone morphogenetic proteins (BMPs) to enhance bone formation has been explored. Bone graft substitutes have been fabricated using freeze drying, solvent casting-porogen leaching, and gas foaming. These traditional techniques cannot control the internal architecture, porosity, and geometry of the scaffold [2]. For bone regeneration, the optimal scaffolds should precisely adopt the bone defect shape and intimately match the

© 2021 The Author(s). Published by IOP Publishing Ltd

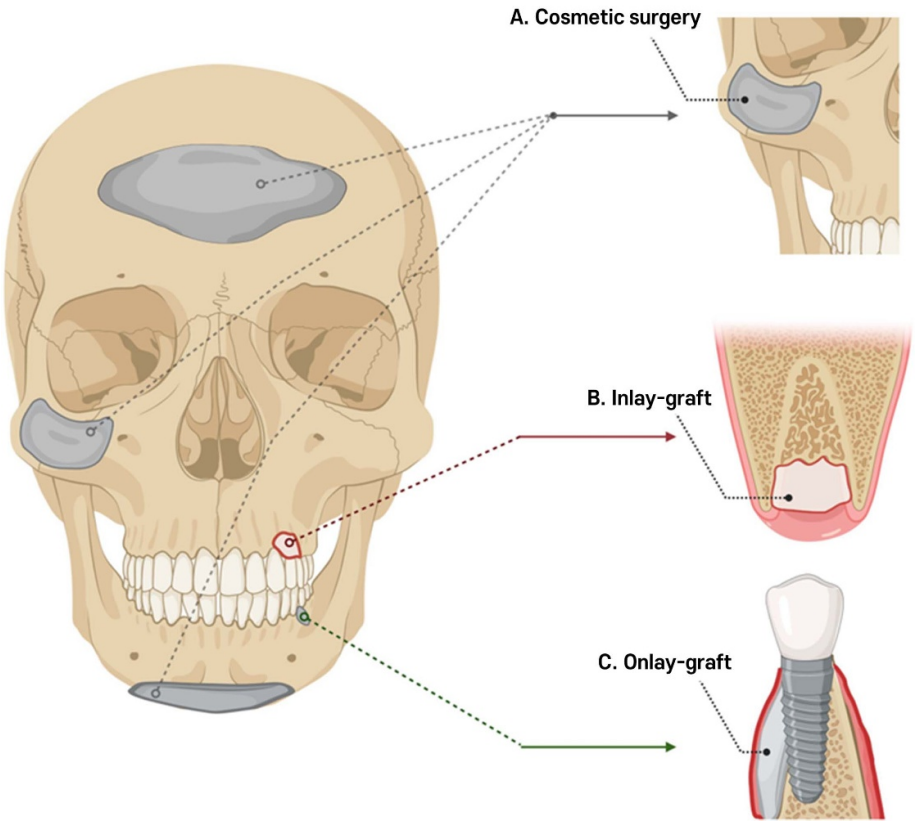

Figure 1. Schematic of graft types in the maxillofacial region. (A) Onlay-graft for cosmetic surgery. (B) Onlay-graft for dental implant. (C) Inlay-graft for extraction socket preservation.

surrounding tissues [3, 4]. Three-dimensional (3D) printing technology has rapidly become a promising alternative to traditional bone graft substitutes, and various alloplastic scaffolds with customized shapes and internal structures have been suggested [5, 6].

Synthetic polymers that could be used as 3D-printed scaffolds include polycaprolactone (PCL), poly(glycolic acid), poly(lactic acid), and poly(lactic-coglycolic acid) [7–9]. PCL is a biodegradable polymer that is widely used because of its malleability, excellent mechanical properties, and support of cell proliferation [10]. In recent study of a complex bone defect in rabbit calvaria, the PCL-Kagome-structure scaffold showed better fitting ability and osteoconductivity compared with the conventional grid-structure [4]. The Kagome-structure is typical and features excellent specific rigidity and a porous microstructure with open pores that can be manufactured by 3D printers [11]. A previous study documented the ability of a Kagome-structure scaffold to adopt a precise shape compared to a scaffold having a general lattice structure [3].

The PASS principle (P: primary closure, A: angiogenesis, S: space maintenance, S: stability) may enable successful bone grafting [12]. An excellent blood supply and stable 3D structure can result in successful bone healing that includes adequate angiogenesis. The onlay-graft is a bone graft procedure in which a transplanted bone substitute is placed directly on the surface of the recipient bone. Patients frequently require onlay-grafts, especially for dental implants and facial plastic or reconstructive surgery, which require increased bone volume. In contrast to the inlay-graft, which is performed inside the bony defect, the onlay-graft has a limited contact area for osteogenic cells and factors, and for angiogenesis factors that are mainly from the adjacent native bone with some from the soft tissue above the graft [13]. Moreover, onlay-grafts protrude from the recipient surface. This requires that the mechanical stability of the bone substitutes should be sufficient to withstand the external dynamic force from the overlying soft tissues (figure 1).

For successful onlay-grafts, conditions needed for bone are intimate contact with the recipient surface, proper stiffness to enable sustainable rigid fixation, proper microstructure that includes porosity to enhance osteoconductivity, and no serious inflammatory and immunologic reactions. The conditions for the surgical procedure include maximal blood circulation on the recipient site with little hematoma, proper flap management to ensure tension-free sutures to avoid wound dehiscence and to prevent flap necrosis caused by excessive stress, and proper suture technique to prevent subsequent tearing of the stitches. Thus, the onlay-graft is still challenging, and

the risk of complications is high. The success of onlay graft surgery is reliant on the type of procedure and experience of the surgeon.

Recombinant human BMP (rhBMP-2) has been manufactured and refined for medical purposes. The United States Food and Drug Administration (FDA) approved rhBMP-2 incorporated in a collagen sponge in 2007 for bone regeneration [1]. Although collagen is widely used as a carrier of rhBMP-2, the water-soluble protein can be rapidly released from collagen by compression, diffusion, and degradation of the collagen in physiological conditions due to its poor mechanical stability [14]. To overcome these problems, many biomaterials have been researched as rhBMP-2 carriers to achieve stable localized rhBMP-2 concentrations for a sufficient period of time [15–17]. Incorporating the rhBMP-2 to the 3D-printed PCL scaffold has been difficult due to hydrophobic property of PCL. Acrylated hyaluronic acid (HA) is a naturally present and high molecular weight polymer with viscoelastic properties. HA has been recently used as a scaffold for rhBMP-2 and human mesenchymal stem cells for bone regeneration [18]. In addition, HA has medicinal value as it is involved in morphogenesis, wound healing, and inflammation [18]. For onlay-grafts, an osteoconductive Kagome-PCL scaffold that incorporates rhBMP-2 into the HA-based hydrogel could act as a dual or sequential delivery system that slowly releases rhBMP-2 and enhances bone formation.

The aims of this study are to explore the onlay-graft use of 3D-printed Kagome-PCL scaffolds for onlay-graft and surgical procedures using a calvarial bone rat model, and to evaluate the results of the onlay-graft with and without rhBMP-2 in the HA-based hydrogel.

2. Material and methods

2.1. Design of Kagome-PCL scaffolds for onlay-graft using micro-computed tomography (micro-CT)

A Kagome-structure model was fabricated as previously described [4, 11]. For 3D modeling of the rat calvaria model, micro-CT scans were acquired of calvaria of 6 week-old male Sprague-Dawley rats using a SOMATOM Sensation 16 16-slice multidetector CT scanner (Siemens AG, Forchheim, Germany). The operating conditions were 120 kV, 220 mA, and 0.75 mm thickness. Axial 0.1 mm-thick views were reconstructed using the CT scanner with a H60s medium-smooth kernel. The field of view was 100 × 100 mm on the bregma (perpendicular intersection of the coronal suture and sagittal suture), and data were acquired in a 512 × 512 data matrix.

PCL (Mw = 43 000, Tm = 55 °C–65 °C; Polysciences, Inc., Warrington, PA, USA) was selected to fabricate the scaffold. The Kagome-structure scaffold was designed using a 3D reconstruction model and CATIA V5 R13 software (Dassault systems®; CATIA, Paris, France). The Kagome-structure model was cut along the outline of the calvarial contour at the coronal view of rat bregma (figure 2(A)). The scaffold was composed of a number of Kagome unit cells. The 3D-Kagome model structure was divided into regions of frames and columns. The cylinder-shape scaffold was 3 mm in height and 5 mm in diameter, with four side wings 1.2 mm in height and 3 mm in diameter, with a porosity of 50% (figure 2(B)).

2.2. 3D printer fabrication of PCL scaffolds with precision extruding deposition (PED) head

Slic3r version 1.2.9 open source software was used for a tool pathway generation of the STL model (figure 3(A)) [11]. The lab-made precision 3D printer with the PED head is shown in figure 3(B). The PED head comprised a barrel, screw, cartridge body, nozzle, gear set, heating block, and motor (figure 3(B)). The structural design of the PED head was improved by a parallel-type gear set. The melted material was extruded by rotating the screw at 45 rpm with an air pressure of 250 ± 5 kPa to prevent heating to a temperature exceeding 88 °C, which is the melting point of the PCL pellet. Several Kagome-structure scaffolds were made simultaneously using a 100 μm ceramic nozzle. The onlay-graft scaffold was constructed in three dimensions by flipping the scaffold, as shown in figure 3(C). The scaffold was turned upside down so that the surface quality of the support location degraded during 3D printing. To intimately match the surface of the rat calvaria, supporters were not created on the curved part of the scaffold. However, the wing part floats in the air when upside down for precise printing of the curved part of the scaffold. To overcome this problem, a support was additionally designed to support the wing part during wing printing, as shown in green portions of figure 3(C). Finally, a scaffold was prepared by removing the support from the prepared scaffold.

2.3. Preparation and surgery process for Kagome-PCL scaffolds with rhBMP-2 loaded in the HA-based hydrogel

HA (MW 170 000 Da) was purchased from Lifecore Biomedical Co. (Chaska, MN, USA). 1-Ethyl-3-(3-dimethylaminopropyl)-carbodimide (EDC), triethanolamine (TEA), and adipic acid dihydrazide (ADH) were acquired from Sigma-Aldrich (St. Louis, MO, USA). 1-Hydroxybenzotriazole hydrate (HOBt) was purchased from Fluka Chemical (Buchs, Switzerland). N-acryloxysuccinimide (NAS) was purchased from Acros Organics (Pittsburgh, PA, USA). Arginylglycylaspartic acid peptides and matrix metalloproteinase (MMP)-insensitive peptides were obtained from AnyGen (Gwang-ju, Korea). Carrier-free rhBMP-2 was purchased from Cowell Medi Co. (Busan, Korea). Fetal bovine serum,

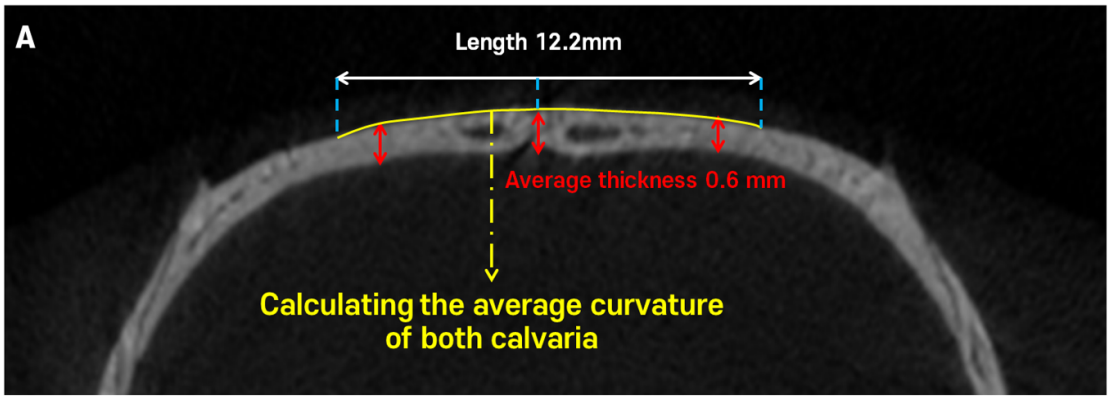

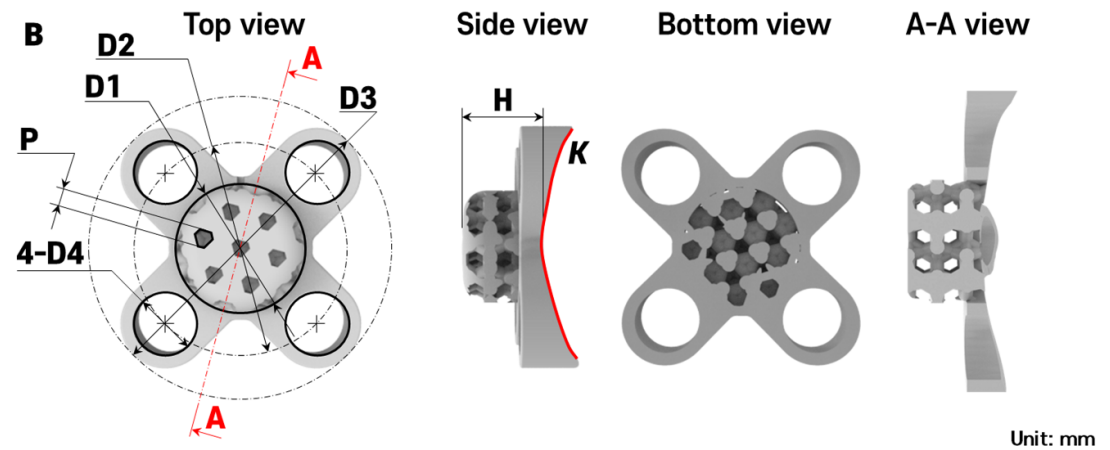

Unit: mm

D1	D2	D3	D4	P	H	K
5	8.6	12.2	2.6	≈ 0.5	3	Rat calvaria

Figure 2. Design of customized PCL scaffold using micro-CT data. (A) Coronal view of bregma calvarial bone in a 7 week-old rat. (B) The 3D design and detailed size of the Kagome-PCL scaffolds with pore size of about 500 micrometers.

penicillin streptomycin, trypsin, and low-glucose Dulbecco's modified Eagle's medium were purchased from GIBCO BRL (Grand Island, NY, USA).

HA (0.25 mmol, based on the repeating unit MW) was dissolved in 40 ml distilled water and EDC (0.24 g, 1.25 mmol), HOBt (0.17 g, 1.25 mmol) and ADH (2.2 g, 12.5 mmol) were added to the solution. The EDC-mediated coupling reaction between the carboxyl group of HA and the hydrazide group of ADH proceeded with continuous stirring at room temperature for 8 h. HA–ADH was dialyzed against 100 mM NaCl for 2.5 d and against distilled water for 1 d using a dialysis membrane (MWCO14,000; SpectraPor, Rancho Dominguez, CA, USA). NAS (0.5 g, 3 mmol) was then added to the HA–ADH solution. The reaction continued with stirring at room temperature for 12 h. HA–ADH–NAS was dialyzed extensively against 100 mM NaCl for 2.5 d and against distilled water for 1 d. The product was lyophilized for 3 d to obtain solid acrylated HA.

For gel preparation, the acrylic HA was dissolved in a TEA-buffered solution (0.3 M, pH 8). MMP-sensitive peptide (GCRDGPQGIWGQDRCG) was loaded in the same molar ratio as the acryl and thiol groups [18]. Polyethylene glycol (PEG)-SH4 (MW 10000) was added as a cross-linker with the same molar ratio as the acryl and thiol groups. The HA-based hydrogel was formed by an additional Michaelis Arbuzov reaction [19]. The reaction mixture was incubated at 37.1 °C for gelation. For animal experiments, 1 μg rhBMP-2 was mixed and reacted with the HA gel [20]. Then, 35 μl of the HA gel reaction mixture was injected into the scaffold using a pipette. For the gelation of HA, the scaffold loaded with the gel in the scaffold was incubated at 37 °C for 30 min. The HA loaded scaffold was implanted immediately after gelation in the calvaria of rats in the Kagome-PCL scaffold containing rhBMP-2/HA (group II).

2.4. Scaffold characterization

Morphology reproducibility of Kagome-PCL scaffold analyzed via a scanning electron microscope (SEM; SU3800, HITACHI, Japan). The prepared scaffold was coated with platinum for 120 s using a sputtering system to prepare for analysis. Platinum-coated scaffolds were fixed on an SEM-specific jig and analyzed in a vacuum chamber.

In addition, in order to analyze the reproducibility of the pores of the fabricated scaffold, pore size

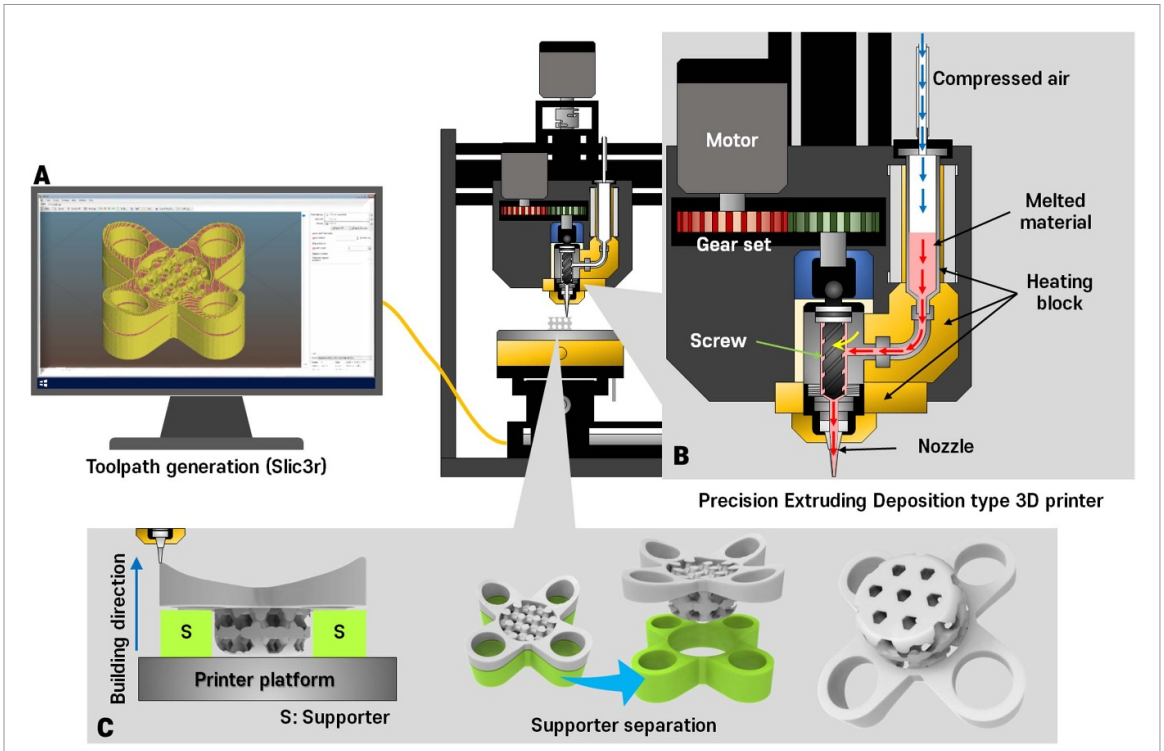

Figure 3. 3D illustration of the Kagome-structure scaffold deposited by 3D printing [11]. (A) Scaffold tool pathway generation using the Slic3r open-source program. (B) Schematic of the developed precision 3D printer and PED head. (C) Schematic of the direction of onlay-graft scaffold construction and the preparation process. Reproduced from [11]. © IOP Publishing Ltd. All rights reserved.

measurement was carried out, and to check whether the HA gel was well mounted inside the fabricated scaffold, it was observed through a digital microscope (Leica; DMS1000, Germany). Five samples were used for measurement, and five points were measured for each sample.

2.5. Animal procedures and surgical installation of Kagome-PCL scaffolds

The animal procedures were approved by the Institutional Animal Care and Use Committee (No. 2019-12-335) and followed the ethical principles for animal experimentation established by the institute. Sample size was initially calculated for 20 animals using six experimental groups, considering a significance level of 5% and a statistical test power of 95%. To rationalize and distribute the animals, we considered 24 animals to be suitable for the experiment. Twenty-four rats were purchased from Orientbio© (Seongnam, Korea) and divided into six groups. The 3 mm height of scaffolds with and without rhBMP-2/HA was determined following sacrifice of rats at 2, 4, and 8 weeks (table 1).

The surgery to install each onlay-graft is summarized in figure 4(A). In more detail, rats were anesthetized by an intramuscular injection of 20 mg of tiletamline and zolazepam hydrocholoride (Zoletil 50®) and xylazine hydrochloride (Rompun®). The hair from the surgery site was shaved, and the site was disinfected with povidone-iodine. After infiltration of

Table 1. Allocation of the male Sprague-Dawley rats.

	Time of sacrifice (weeks)		
Male Sprague rats	2	4	8
3 mm Kagome-PCL scaffold			
Group I (without rhBMP-2/HA)	$N = 4$	$N = 4$	$N = 4$
Group II (with rhBMP-2/HA)	$N = 4$	$N = 4$	$N = 4$

1.8 ml of 2% lidocaine HCl (Huons®, Kyeongi-do, Korea) for local anesthesia, a linear incision was made from the distal margin of the scaffold along the sagittal line, and the periosteal was anteriorly dissected to form a pocket beneath (figures 4(B)–(D)). Three to four foramina were made for decortication with a micro-drill (2.0 mm diameter; Neobiotech, Seoul, Korea) at the bregma [21] (figure 4(E)). The scaffold was positioned on the bregma and fixed using miniscrews (4 mm long, 2 mm diameter; Neobiotech) on the four side wings (figure 4(F)). During drilling, the site was irrigated with sterile saline to prevent thermal damage. After flap adaptation, the scaffold was covered with non-damaged soft tissue (figure 4(G)). The surgical site was sutured using a continuous horizontal mattress suture technique and a vertical mattress suture on the anterior third of incision line with 4–0 black silk (figures 4(H) and (I)).

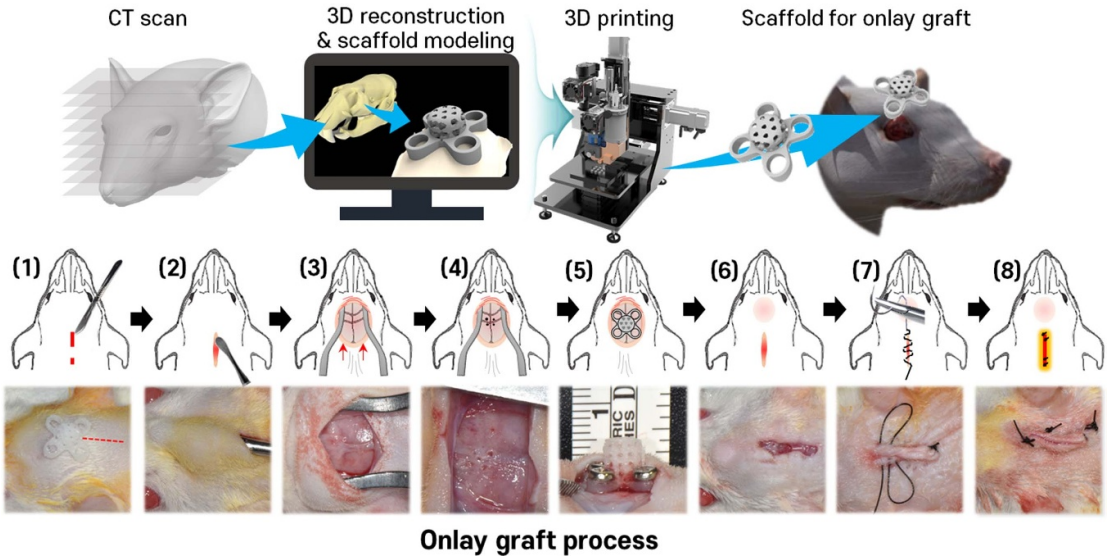

Figure 4. Onlay-graft process with 3D printed Kagome-PCL scaffold on rat calvarial bone. Schematic of the onlay-graft process with 3D printed Kagome-structure PCL scaffold. (1) The incision line (red line) is made at posterior point on the scaffold. (2) Anterior dissection of the periosteum flap is made toward the bregma. (3) The bregma is exposed. (4) Decortication is done with three to four holes drilled in the bregma. (5) The scaffold is adapted on the bregma and fixed with four miniscrews. (6) The flap fully covers the scaffold without including the incision line. (7), (8) Continuous horizontal mattress sutures and vertical mattress sutures are made on the anterior third of the incision line using 4–0 black silk.

Following the surgery, cefazolin (50 mg kg^{-1}) and ketorolac tromethamine (1 mg kg^{-1}) were administrated intramuscularly twice daily for 3 d to reduce pain and to prevent infection. The site was disinfected with povidone-iodine solution.

2.6. Micro-CT analysis

After sacrifice, the scaffold was carefully excised *en bloc* with calvarial bone using a saw after incision and dissection of skin and subcutaneous tissue (figure 6). The removed tissues were immediately fixed in 4% (w/v) paraformaldehyde and stored for 5 d. The grafts were obtained by removing the fixation screws after sacrifice. Micro-CT scans were acquired as described earlier in the text. Fixed specimens were wrapped with parafilm to minimize drying. The specimens were scanned by micro-CT using a model 1176 device (SkyScan, Kontich, Belgium) at a high resolution with an aluminum filter (0.5 mm). Scan settings were as follows: resolution of 35.76 μm pixels, energy of 50 kV, and intensity of 500 μA. Projection images of CT scans and reconstructions were saved as 16-bit TIFF files. The image files were transferred to set the measurement software (CTVox; Blue Scientific, Cambridge, UK).

To compare the degree of bone formation *in vivo*, CT scans were acquired each week. The new bone volume and scaffold shape retention were qualitatively measured by 3D reconstruction using Materialise v 21.0 (MIMICS, Leuven, Belgium). This program integrates CT data composed of tomographic images to reconstruct a 3D model. First, 3D modeling was performed by integrating CT data of pure rat calvaria from the negative control for the reference shape. Then, to measure the volume of the new bone, only the new bone was isolated and reconstructed into a 3D model. Briefly, referring to the reconstructed pure rat calvaria 3D model, the original bone area was removed and only the remaining area was reconstructed into the 3D model. The volume of the isolated new bone was measured as CAD data in the MIMICS program. The bone formation ratio was calculated from the measurement data per total cavity volume (35 μl) of the 3 mm Kagome-PCL scaffold.

2.7. Histological analyses

After micro-CT scan acquisition, decalcification was performed using 10% ethylenediaminetetraacetic acid for 28 d at room temperature. The prepared samples were embedded in paraffin after dehydration. Coronal sections (4 μm in thickness) were stained with hematoxylin and eosin and Masson's Goldner trichrome to evaluate angiogenesis, new bone formation, and spatial gap between the scaffold and calvarial bone. In addition, the height of the scaffold was measured using histologic images to evaluate the maintenance of the shape of each sample. The height was calculated as the average height of five points on top of the scaffold per sample.

2.8. Statistical analysis

All data are expressed as the mean ± standard deviation. Statistical analysis was performed on the micro-CT results using single factor analysis of variance with SPSS version 25.0 software (SPSS, Inc., Chicago, IL, USA). Significance was considered at a level of 0.05.

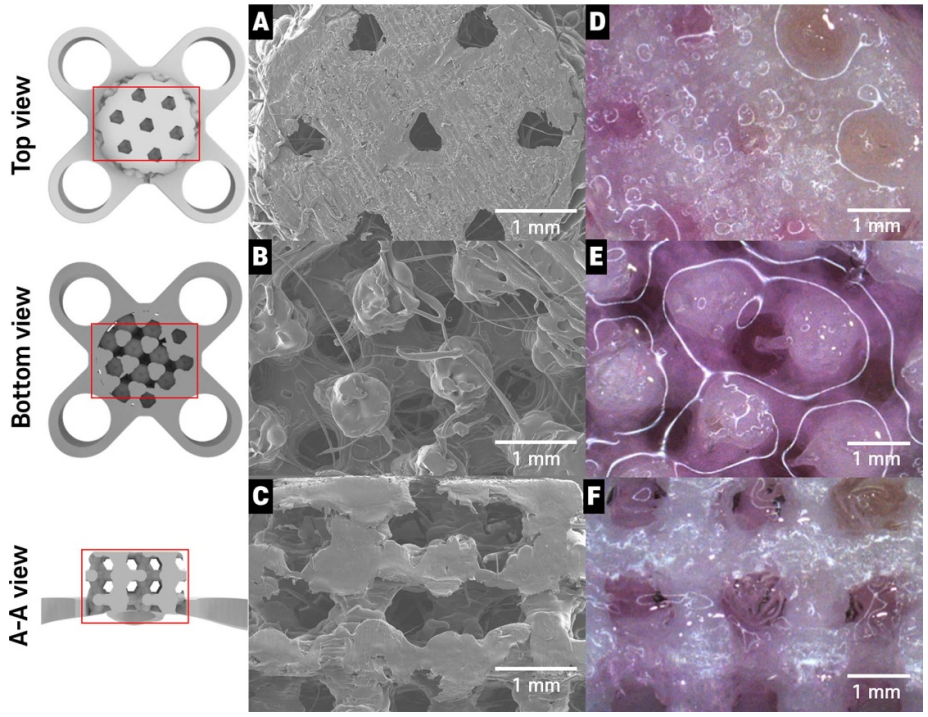

Figure 5. SEM and digital microscope images of the 3D printed Kagome-PCL scaffold. (A) Top view, (B) bottom view, and (C) cross section view of SEM images. (D) Top view, (E) bottom view, (F) cross section view of optical microscope images.

3. Results

The fabrication reproducibility of the Kagome-PCL scaffold was confirmed in figure 5. Figures 5(A)–(C) confirmed the fabrication reproducibility of the scaffold through SEM. Through the SEM images (A. top view, B. bottom view, C. cross section view), it can be confirmed that the open pore and pore interconnected kagome structures are well implemented. The realization of the pore size of the fabricated scaffold was measured through a digital microscope, which was measured to be an average of 524.34 ± 9.62 μm. In addition, it was confirmed that the interior of the scaffold manufactured by HA was well mounted, as shown in figures 5(D)–(F).

The 3D-printed Kagome-PCL scaffolds were fabricated for an intimate surface fit. No dehiscence, swelling, or hematoma was evident in any rat during the observation period (figure 6(A)). At sacrifice and removal of the fixation screws, all scaffolds were well-integrated with the calvarial bone with fibrous tissue coverage (figure 6(B)).

3.1. Micro-CT results

CTVox software was used to analyze bone formation within the Kagome-PCL scaffold in CT images. The differences in bone formation in groups I and II are shown in figures 7 and 8 and table 2.

3.2. Histologic results

Close contact was formed between the Kagome-PCL scaffold and the calvarial bone. The close contact did not allow invasion of any soft tissue to the surface. Dense fibrous tissues were integrated from the lateral and coronal sides of the PCL scaffold at the early stage (2 weeks) regardless of the absence or presence of rhBMP-2/HA. New bone formation was observed from the calvarial bone below the scaffold, and active bone remodeling was evident around the decorticated holes. The roofs (third columns) of all the scaffolds were well-maintained without collapse in all samples.

The histological differences in bone formation in groups I and II are shown in figure 9.

The height of the scaffolds was measured (table 3 and figure 10) and were found to be approximately 3 mm (max error rate 2.14%; approximately <65 μm). There was no significant change in the height of the scaffolds.

4. Discussion

Successful onlay-graft outcome requires that the graft material be placed at the recipient site as tightly as possible. In addition, considering the unique nature of the onlay-graft, the shape and size of the graft material should be maintained over time.

Maxillofacial bony defects have complex curvatures, which makes it difficult to achieve tight contact between the recipient site and the conventional graft. The result can be malunion or displacement of the graft. The current 3D printing technology can fabricate bone graft materials with a customized size and shape for such complex

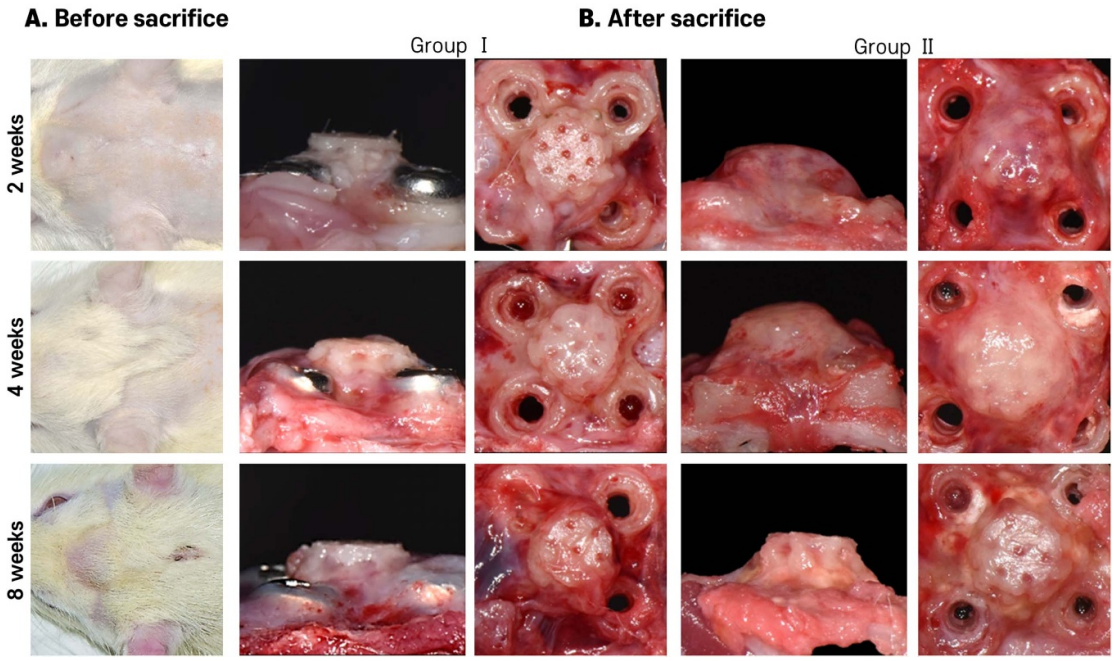

Figure 6. Clinical photographs before and after sacrifice. (A) Complete healing of incision sites of all rats without wound dehiscence was observed. (B) Appearance of grafts after sacrifice and removal of all fixation screws. Scaffolds without and with rhBMP-2/HA were covered with fibrous tissue and were well-integrated with the calvarial bone.

conditions. This is a marked improvement over the classical types of bone grafts. Tight contact between the graft and the recipient site enhances the speed of bone engraftment due to faster vascularization and cellular migration. In addition, the intimate contact could also improve graft stability at the recipient site, which could enhance the graft success rate [13, 22]. In our previous study [4], we showed that in the inlay-graft condition, the positions of the 3D-printed Kagome-PCL grafts were far more stably maintained with time than that of the conventional 3D printed grid-type PCL graft because of the tighter contact of the Kagome type at the recipient site.

Studies have sought to engineer scaffolds by considering solvent casting, fiber bonding, phase separation, gas-induced foaming, and salt leaching to mimic the complex geometries of the human body [23]. Among them, PED with a mechanical screw dispensing system was developed to fabricate more delicate PCL scaffolds [24]. This involved the extrusion of a highly viscous material through a small-diameter nozzle (<100 μm diameter), and desired mechanical properties, structural integrity, and controlled pore size and interconnectivity [3, 11, 24]. In this study, using this technique, 3D-printed Kagome-PCL scaffolds were accurately manufactured to meet the needs for mechanical strength and delicate structure (figures 7(A) and 8(A)).

The scaffold height was designed to be 3 mm since a graft height of at least 2 mm is required for cosmetic surgery [13, 25]. Continuous pressure over the graft from overlying soft tissues, such as muscle, skin, or mucosa, might cause graft resorption and displacement, with an unsatisfactory result. Therefore, the absorbable graft should endure the overlying soft tissue pressure without change of the graft height and shape until newly regenerated bone replaces the graft materials as the graft gradually degrades with time [1]. In this study, similar with our previous studies [4, 11], the Kagome graft had sufficient mechanical strength to resist overlying pressure in the critical period. Collapse was not observed in any sample, and new bone grew well from the surface of the recipient native bony surface to the graft (table 2).

Wound dehiscence at the graft site is the most frequent cause of graft failure of bone grafts [26]. In particular, an onlay-graft increases the possibility of wound rupture because the excess volume of the graft could extend to overlying soft tissues [22]. Once wound dehiscence occurs, the graft material is exposed and is infected. Thus, a careful surgical design is important to prevent wound dehiscence. In this study, the skin incision was performed to cover the graft by non-damaged soft tissue. No wound dehiscence or graft failure occurred in any of the rats in this study.

PCL is a popular material for 3D-printed bone graft materials [7]. It is degraded by the hydrolysis of its ester linkages in the human body and has therefore received great attention for use as an implantable biomaterial. PCL has been approved by the US FDA for specific human applications that include drug delivery, suture, or as an adhesion barrier [27]. However, PCL suffers from some tissue engineering pitfalls that

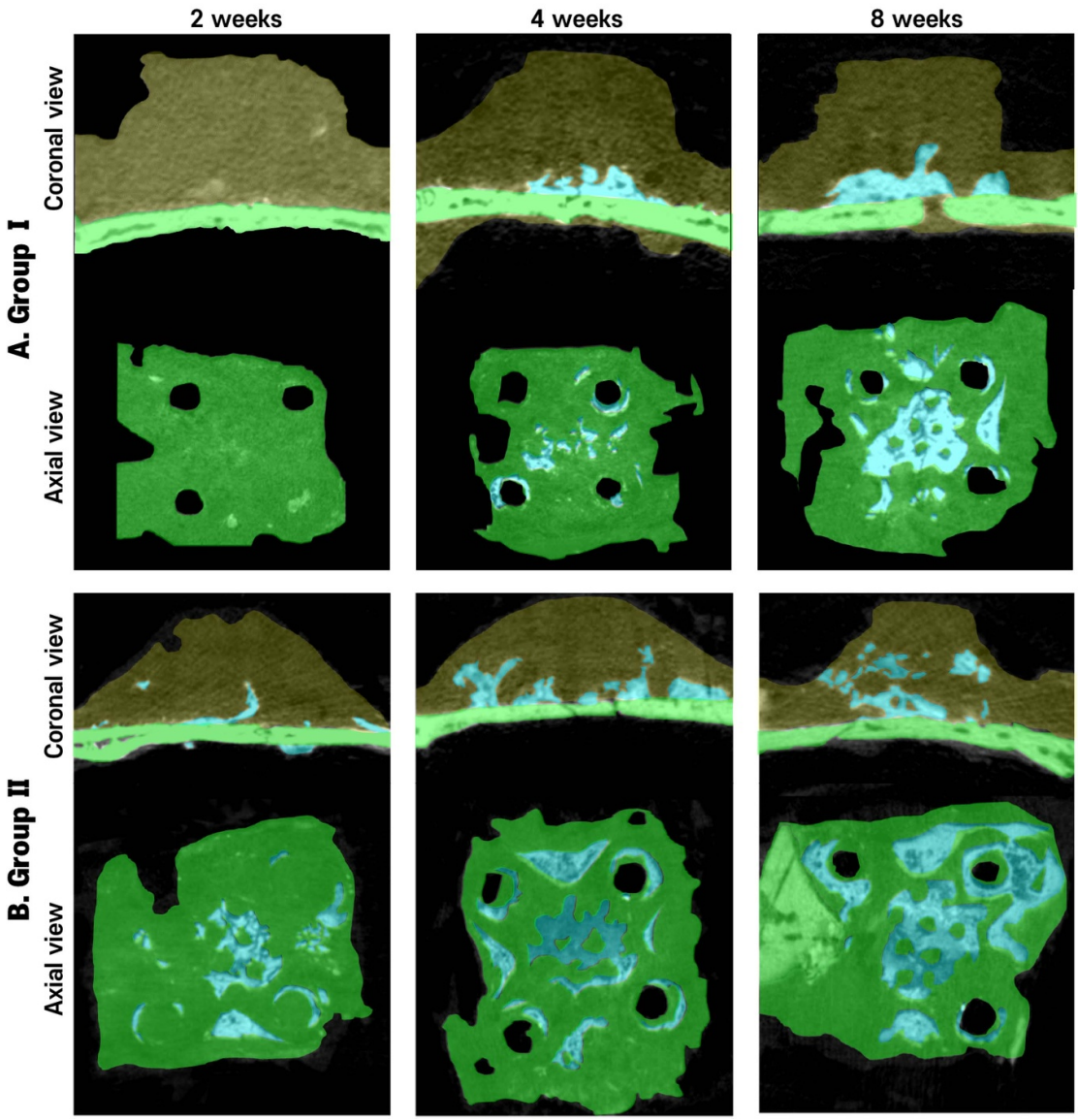

Figure 7. Micro-CT images of the Kagome-PCL scaffold grafts without and with rhBMP-2/HA. The measurement of new bone volume (highlighted in cyan). The bone volume was calculated by integrating bone tissue located inside the scaffold and above the calvarial bone. (A) Results for group I. New bone formation was not evident at 2 weeks. At 4 weeks, new bone formation was slightly evident inside the scaffold. At 8 weeks, new bone formation was observed in almost the entire first column cavity. The axial view of the scaffold revealed the Kagoma-shape of the newly formed bone in the scaffold at 8 week. (B) Results for group II. At 2 weeks, new bone formation was slightly observed inside the scaffold, and was superior to that of group I at 4 weeks. At 4 weeks, new bone formation was observed in almost the entire first column cavity of the scaffold. At 8 weeks, new bone formation was observed in almost the entire second column cavity of the scaffold. The axial view of the scaffold revealed the Kagoma-shape of the newly formed bone inside the scaffold beginning at 2 weeks postoperatively.

include slow degradation rate, poor mechanical properties, and poor cell adhesion [26].

To overcome the limitations of PCL for bone regeneration, rhBMP-2 was incorporated into the grafts. rhBMP-2 is a potent growth factor that enhances the osteoblastic differentiation of stem cells, angiogenesis, and new bone formation. Maintaining an adequate concentration of rhBMP-2 at the graft site for a required period of time is essential for graft success because of its short biological half-life, water-soluble property, and rapid clearance [14–16]. Therefore, a proper carrier of rhBMP-2 may be critical for its successful use. Recently, to regulate the expression and concentration of rhBMP-2, several hydrogels have been developed as a delivery scaffold. They include HA [18], crosslinking of aqueous gelatin with glutaraldehyde [28], and functional nanoparticle–hydrogel complexes [29]. In particular, hydrogels are hydrophilic hydrated polymers that easily deliver oxygen and nutrients to tissues [30]. The hydrophilic properties allow incorporation of rhBMP-2 and other water-soluble growth factors into hydrophobic polymer scaffolds like PCL. HA, a biologically active molecule that regulates the tissue repair process

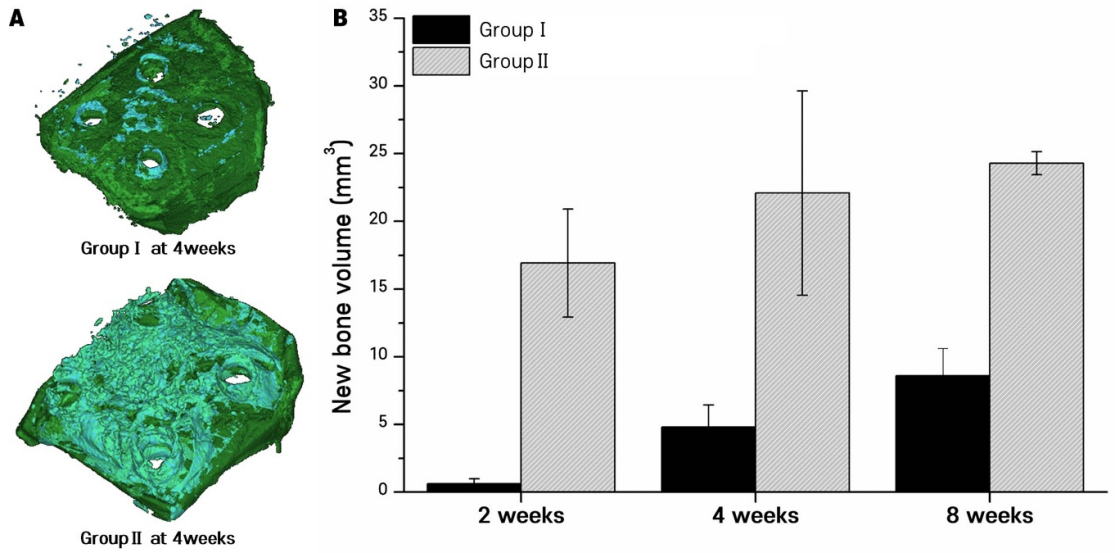

Figure 8. Measurement of new bone volumes. The bone volume was calculated by integrating bone tissue located inside the scaffold and above the calvarial bone (highlighted in cyan color). (A) Appearance at 4 weeks for group I (top) and group II (bottom). (B) Volume comparison of calculated new bone at 2, 4, and 8 weeks.

Table 2. Ratio of new bone/cavity of the Kagome-PCL scaffold without and with rhBMP-2/HA.

	2 weeks	4 weeks	8 weeks	P^*
New bone formation (ratio, %)				
Group I (without rhBMP-2/HA)	1.76 ± 1.06	13.74 ± 4.66	24.57 ± 5.78	2 vs 4: 0.002
				4 vs 8: 0.066
				2 vs 8: <0.001
Group II (with rhBMP-2/HA)	48.34 ± 1.14	63.13 ± 2.16	69.38 ± 2.44	2 vs 4: 0.353
				4 vs 8: 0.644
				2 vs 8: 0.035
$P^\dagger$	<0.001	<0.001	<0.001	

Independent-sample *t*-test between the sacrifice weeks (*) and the groups (†).

on multiple levels, also showed a positive effect on wound healing [31]. Benefits of HA in both early and late wound healing have been described [32, 33]. A recent study documented that HA hydrogels promoted comparable skin-wound healing outcomes with basic fibroblast growth factor [34]. In addition, HA-incorporated composite scaffolds showed great potential for enhancing osteogenesis and mineralization, and as local delivery carriers for osteoinductive components [35]. Concerning our results, an HA hydrogel could enhance bone regeneration and prevent wound dehiscence, which is the most common complication of the onlay-graft [13].

Our histological and radiological results also indicate a synergistic effect of the Kagome-PCL scaffold and HA hydrogel. This dual scaffold could deliver rhBMP-2 slowly and consistently without degeneration, which is supported by the observations of gradual angiogenesis and retention of HA through 8 weeks (figure 9(B)). In this study, the 3 mm Kagome-PCL scaffold could endure external forces from the overlying soft tissue for 8 weeks *in vivo*. New bone formed in the first column cavity of the scaffolds in group I at 8 weeks. However, the amount of new bone at 8 weeks in group I (24.57%) was significantly less than that in group II at 2 weeks. The new bone occupied approximately 48.4% and 69.5% of the total cavity volume of the scaffolds containing rhBMP-2/HA at 2 and 8 weeks, respectively.

In this study, HA remained during the resorption that occurred for up to 8 weeks. In the *in vivo* environment, as the MMP-sensitive peptide cross-linker in the HA-based hydrogel is degraded by the surrounding cells, the stiffness of the hydrogel is gradually reduced. Thus, the exposure rate of the hydrogel to the surrounding tissue is important in determining the degradation speed of HA. With this in mind, the design of the Kagome-PCL scaffold could be considered more advantageous as a container to induce the delayed degradation of the HA-based hydrogel than the conventional grid-structure scaffold. In our

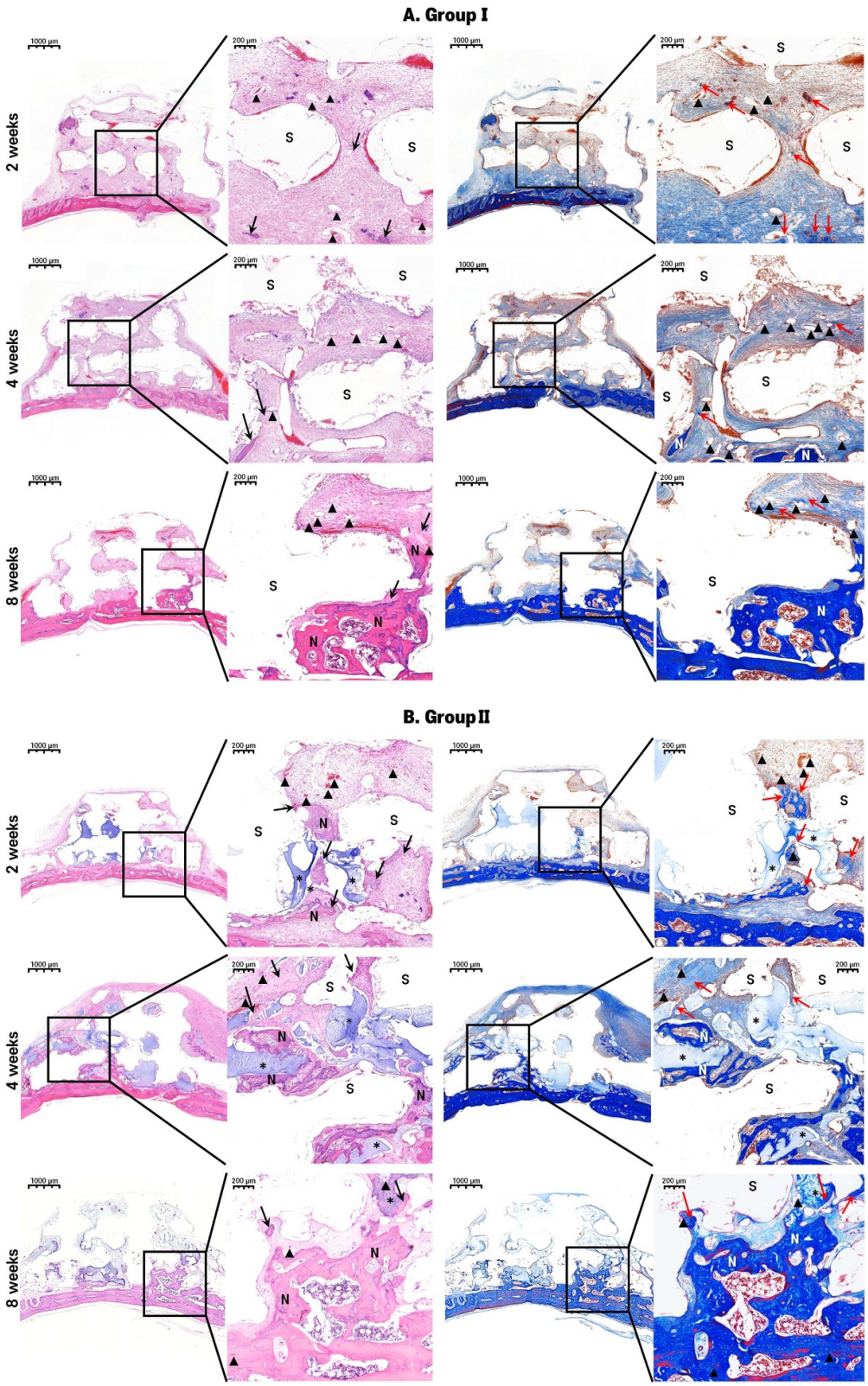

Figure 9. Hematoxylin and eosin and Masson's Goldner trichrome staining of onlay-grafts with the Kagome-PCL scaffold without and with rhBMP-2/HA. (A) Histological results of group I. At 2 weeks, the angiogenesis and dense collagen bundles were observed on the second column cavity of the scaffold. New bone formation was observed at 4 weeks from the calvarial bone. At 8 weeks, new bone had grown to the first column cavity of the scaffold. (B) Histological results of group II. New bone formation was observed at 2 weeks from the calvarial bone with dominant angiogenesis and dense collagen bundle. The new bone, vessels, and collagen bundles were more dense at 4 weeks. HA-based hydrogel remained around the new bone. At 8 weeks, the new bone was mature. The remaining HA displayed resorption and was replaced with newly formed bone matrix. (Asterisk, HA-based hydrogel; arrow, new bone matrix; arrowhead, new blood vessel; S, scaffold; N, new bone; HA, hyaluronic acid; rhBMP-2, recombinant human bone morphogenetic protein.)

Table 3. Average height of the Kagome-PCL scaffold without and with rhBMP-2/HA.

	2 weeks	4 weeks	8 weeks
Average height of the scaffold (mm)			
Group I (without rhBMP-2/HA)	3.03 ± 0.09	3.02 ± 0.14	3.01 ± 0.11
Group II (with rhBMP-2/HA)	3.06 ± 0.08	3.02 ± 0.10	3.02 ± 0.06

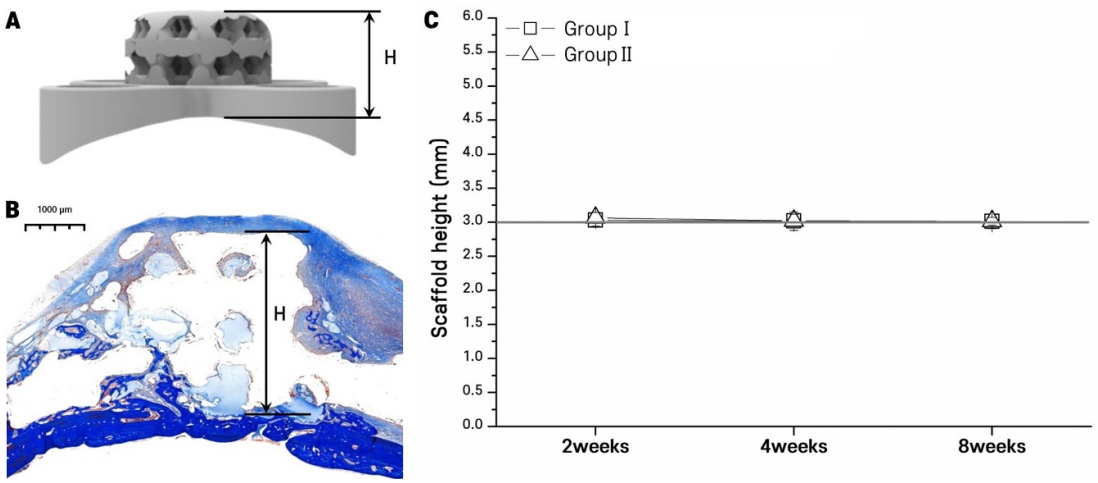

Figure 10. Scaffold height measurement data from Masson's Goldner trichrome stained images.

preliminary study, the HA-based hydrogel degraded at a much slower rate in the Kagome-PCL scaffold than in the conventional grid scaffold, even though the porosity ratio was the same in both scaffolds. This might be because the total surface area of the hydrogel that is exposed to surrounding tissue is only about 26% in the Kagome-PCL scaffold but about 90% in the conventional grid type scaffold (data not shown).

The effective delivery of rhBMP-2 and synergistic effect by the Kagome-PCL scaffold/HA hydrogel system could be crucial in the onlay-graft procedure, which has high risks of wound dehiscence and lack of osteogenic cells from recipient bone. Also, as excessive dose of rhBMP-2 has often adverse effect, this slow release feature of rhBMP-2 in the Kagome-PCL scaffold with HA hydrogel could have additional benefit of reduction the therapeutic dose and side effects of rhBMP-2 while maintaining bone healing potency [14].

Further studies are needed to reveal the duration and release profile of rhBMP-2 with this dual scaffold. These studies should include assessments of the postulated release profile of bigger rhBMP-2/HA containing Kagome-PCL scaffolds in animal experiments of larger sample size. After verifying the release profile of this dual scaffold, the optimal condition for clinical application should be determined, including the concentration of rhBMP-2, porosity of the Kagome-structure, and maximum size of the Kagome-PCL scaffold.

5. Conclusion

All 3D-printed Kagome-PCL scaffolds were accurately placed and firmly integrated to the recipient bone. Micro-CT and histology analyses revealed the maintenance of the height of the scaffolds in all animals, confirming the sufficient mechanical strength of the scaffold. In addition, 3D-printed Kagome-PCL scaffolds maintained rhBMP-2 mixed in HA during the observation period. Newly formed bone in the scaffold was observed in the absence (group I) and presence (group II) of rhBMP-2 mixed in HA. New bone volume was greater in group II. These results suggest the promising clinical feasibility of the 3D-printed Kagome-PCL scaffold for use in onlay-graft procedures.

Data availability statement

The data generated and/or analyzed during the current study are not publicly available for legal/ethical reasons but are available from the corresponding author on reasonable request.

Acknowledgments

We thank the Laboratory of animal research core facility at the Convergence Medicine Research Center (CREDIT), Asan Medical Center, for support and instrumentation.

Part of the figure Created with BioRender.com (Agreement number:DI22LU9CFV).

Funding

This research was supported by a grant from the Korea Health Technology R&D Project through the Korea Health Industry Development Institute (KHIDI), funded by the Ministry of Health & Welfare, Republic of Korea (Grant Number: HI14C2143).

Author contributions

Jeong-Kui Ku performed surgery, analyzed the data, and wrote the manuscript. Kang Gon Lee manufactured the HA hydrogel with rhBMP-2, performed data analysis, and wrote the manuscript. Min-Soo Ghim manufactured the 3D printed Kagome-structure PCL scaffold, analyzed the data, and wrote the manuscript. Young-Kyun Kim provided advice concerning the scaffold application. Sang-Hyug Park provided advice concerning the scaffold fabrications. Yongdoo Park supervised the study and provided critical discussion for the HA hydrogel with rhBMP-2. Young-Sam Cho supervised the study and provided critical discussion of the 3D printed Kagome-structure PCL scaffold. Bu-Kyu Lee conceived the study determined the shape of the scaffold, administered and supervised the study, and wrote the manuscript.

Conflicts of interest

There are no conflicts of interest to declare.

ORCID iDs

Jeong-Kui Ku https://orcid.org/0000-0003-1192-7066
Kang-Gon Lee https://orcid.org/0000-0003-0026-616X
Min-Soo Ghim https://orcid.org/0000-0001-1192-7066
Young-Kyun Kim https://orcid.org/0000-0002-7268-3870
Sang-Hyug Park https://orcid.org/0000-0002-2293-2285
Yongdoo Park https://orcid.org/0000-0003-3822-4651
Young-Sam Cho https://orcid.org/0000-0002-0545-1586
Bu-Kyu Lee https://orcid.org/0000-0001-8888-1719

References

[1] Gomez-Barrena E *et al* 2018 A multicentric, open-label, randomized, comparative clinical trial of two different doses of expanded hBM-MSCs plus biomaterial versus iliac crest autograft, for bone healing in nonunions after long bone fractures: study protocol *Stem Cells Int.* **2018** 1–13

[2] Roseti L, Parisi V, Petretta M, Cavallo C, Desando G, Bartolotti I and Grigolo B 2017 Scaffolds for bone tissue engineering: state of the art and new perspectives *Mater. Sci. Eng.* C **78** 1246–62

[3] Lee K-G, Lee K-S, Kang Y-J, Hwang J-H, Lee S-H, Park S-H, Park Y, Cho Y-S and Lee B-K 2018 Rabbit calvarial defect model for customized 3D-printed bone grafts *Tissue Eng. Part C Methods* **24** 255–62

[4] Lee S-H, Lee K-G, Hwang J-H, Cho Y S, Lee K-S, Jeong H-J, Park S-H, Park Y, Cho Y-S and Lee B-K 2019 Evaluation of mechanical strength and bone regeneration ability of 3D printed kagome-structure scaffold using rabbit calvarial defect model *Mater. Sci. Eng.* C **98** 949–59

[5] Jammalamadaka U and Tappa K 2018 Recent Advances in Biomaterials for 3D Printing and Tissue Engineering *J. Funct. Biomater.* **9** 22

[6] Thavornyutikarn B, Chantarapanich N, Sitthiseripratip K, Thouas G A and Chen Q 2014 Bone tissue engineering scaffolding: computer-aided scaffolding techniques *Prog. Biomater.* **3** 61–102

[7] Serra T, Planell J A and Navarro M 2013 High-resolution PLA-based composite scaffolds via 3D printing technology *Acta Biomater.* **9** 5521–30

[8] Bose S, Vahabzadeh S and Bandyopadhyay A 2013 Bone tissue engineering using 3D printing *Mater. Today* **16** 496–504

[9] Chia H N and Wu B M 2015 High-resolution direct 3D printed PLGA scaffolds: print and shrink *Biofabrication* **7** 015002

[10] Park S A, Lee S H and Kim W D 2011 Fabrication of porous polycaprolactone/hydroxyapatite (PCL/HA) blend scaffolds using a 3D plotting system for bone tissue engineering *Bioprocess Biosyst. Eng.* **34** 505–13

[11] Lee S-H, Cho Y S, Hong M W, Lee B-K, Park Y, Park S-H, Kim Y Y and Cho Y-S 2017 Mechanical properties and cell-culture characteristics of a polycaprolactone kagome-structure scaffold fabricated by a precision extruding deposition system *Biomed. Mater.* **12** 055003

[12] Wang H and Boyapati L 2006 "PASS" principles for predictable bone regeneration *Implant Dentistry* **15** 8–17

[13] Kim Y and Ku J 2020 Ridge augmentation in implant dentistry *J. Korean Assoc. Oral Maxillofac. Surg.* **46** 211–7

[14] James A W, LaChaud G, Shen J, Asatrian G, Nguyen V, Zhang X, Ting K and Soo C 2016 A review of the clinical side effects of bone morphogenetic protein-2 *Tissue Eng. Part B Rev.* **22** 284–97

[15] Kolk A, Handschel J, Drescher W, Rothamel D, Kloss F, Blessmann M, Heiland M, Wolff K and Smeets R 2012 Current trends and future perspectives of bone substitute materials–from space holders to innovative biomaterials *J. Cranio-Maxillofac. Surg.* **40** 706–18

[16] Um I-W, Ku J-K, Lee B K, Yun P-Y, Lee J K and Nam J-H 2019 Postulated release profile of recombinant human bone morphogenetic protein-2 (rhBMP-2) from demineralized dentin matrix *J. Korean Assoc. Oral Maxillofac. Surg.* **45** 123

[17] Um I-W, Ku J-K, Kim Y-K, Lee B-K and Leem D H 2020 Histological review of demineralized dentin matrix as a carrier of rhBMP-2 *Tissue Eng. Part B Rev.* **26** 284–93

[18] Kim J, Kim I S, Cho T H, Lee K B, Hwang S J, Tae G, Noh I, Lee S H, Park Y and Sun K 2007 Bone regeneration using hyaluronic acid-based hydrogel with bone morphogenic protein-2 and human mesenchymal stem cells *Biomaterials* **28** 1830–7

[19] Jin R, Teixeira L S, Krouwels A, Dijkstra P J, van Blitterswijk C, Karperien M and Feijen J 2010 Synthesis and characterization of hyaluronic acid–poly (ethylene glycol) hydrogels via Michael addition: an injectable biomaterial for cartilage repair *Acta Biomater.* **6** 1968–77

[20] Mumcuoglu Guvenc D, Fahmy-Garcia S, Ridwan Y, Nickel J, Farrell E, Kluijtmans S and van Osch G 2018 Injectable

BMP-2 delivery system based on collagen-derived microspheres and alginate induced bone formation in a time-and dose-dependent manner *Eur. Cell Mater.* **35** 242–54

[21] Danesh-Sani S, Tarnow D, Yip J and Mojaver R 2017 The influence of cortical bone perforation on guided bone regeneration in humans *Int. J. Oral Maxillofac. Surg.* **46** 261–6

[22] Kim Y-K and Ku J-K 2020 Guided bone regeneration *J. Korean Assoc. Oral Maxillofac. Surg.* **46** 361–6

[23] Beheshtizadeh N, Lotfibakhshaiesh N, Pazhouhnia Z, Hoseinpour M and Nafari M 2020 A review of 3D bio-printing for bone and skin tissue engineering: a commercial approach *J. Mater. Sci.* **55** 3729–49

[24] Shor L, Güçeri S, Chang R, Gordon J, Kang Q, Hartsock L, An Y and Sun W 2009 Precision extruding deposition (PED) fabrication of polycaprolactone (PCL) scaffolds for bone tissue engineering *Biofabrication* **1** 015003

[25] Khorasani M, Janbaz P and Rayati F 2018 Maxillofacial reconstruction with Medpor porous polyethylene implant: a case series study *J. Korean Assoc. Oral Maxillofac. Surg.* **44** 128–35

[26] Hajiali F, Tajbakhsh S and Shojaei A 2017 Fabrication and properties of polycaprolactone composites containing calcium phosphate-based ceramics and bioactive glasses in bone tissue engineering: a review *Polym. Rev.* **58** 164–207

[27] Kariduraganavar M Y, Kittur A A and Kamble R R 2014 Chapter 1 - Polymer Synthesis and Processing *Natural and Synthetic Biomedical Polymers Kumbar S G*, Laurencin C T and Deng M 1–31

[28] Reddy N, Reddy R and Jiang Q 2015 Crosslinking biopolymers for biomedical applications *Trends Biotechnol.* **33** 362–9

[29] Heo D N, Ko W-K, Bae M S, Lee J B, Lee D-W, Byun W, Lee C H, Kim E-C, Jung B-Y and Kwon I K 2014 Enhanced bone regeneration with a gold nanoparticle–hydrogel complex *J. Mater. Chem.* B **2** 1584–93

[30] Dong L, Wang S-J, Zhao X-R, Zhu Y-F and Yu J-K 2017 3D- printed poly(ε-caprolactone) scaffold integrated with cell-laden chitosan hydrogels for bone tissue engineering *Sci. Rep.* **7** 13412

[31] Litwiniuk M, Krejner A, Speyrer M S, Gauto A R and Grzela T 2016 Hyaluronic acid in inflammation and tissue regeneration *WOUNDS* **28** 78–88

[32] Gaston J and Thibeault S L 2013 Hyaluronic acid hydrogels for vocal fold wound healing *Biomatter* **3** e23799

[33] Walimbe T, Panitch A and Sivasankar P M 2017 A review of hyaluronic acid and hyaluronic acid-based hydrogels for vocal fold tissue engineering *J. Voice* **31** 416–23

[34] Li X, Li A, Feng F, Jiang Q, Sun H, Chai Y, Yang R, Wang Z, Hou J and Li R 2019 Effect of the hyaluronic acid-poloxamer hydrogel on skin-wound healing: *in vitro* and *in vivo* studies *Anim. Model Exp. Med.* **2** 107–13

[35] Zhai P, Peng X, Li B, Liu Y, Sun H and Li X 2020 The application of hyaluronic acid in bone regeneration *Int. J. Biol. Macromol.* **151** 1224–39